7-21-2023

Excavation response analysis of prefabricated recyclable support structure for water-rich silt foundation pit

Rui-song WANG
School of Civil Engineering, Sun Yat-Sen University, Guangzhou, Guangdong 510275, China, Southern Marine Science and Engineering Guangdong Laboratory (Zhuhai), Zhuhai, Guangdong 519080, China, Guangdong research center for underground space exploitation technology, Guangzhou, Guangdong 510275, China

Cheng-chao GUO
School of Civil Engineering, Sun Yat-Sen University, Guangzhou, Guangdong 510275, China, Southern Marine Science and Engineering Guangdong Laboratory (Zhuhai), Zhuhai, Guangdong 519080, China, Guangdong research center for underground space exploitation technology, Guangzhou, Guangdong 510275, China, Southern Institute of Infrastructure Testing and Rehabilitation Technology, Huizhou, Guangdong 516000, China

Pei-yuan LIN
School of Civil Engineering, Sun Yat-Sen University, Guangzhou, Guangdong 510275, China, Southern Marine Science and Engineering Guangdong Laboratory (Zhuhai), Zhuhai, Guangdong 519080, China, Guangdong research center for underground space exploitation technology, Guangzhou, Guangdong 510275, China

Fu-ming WANG
School of Civil Engineering, Sun Yat-Sen University, Guangzhou, Guangdong 510275, China, Southern Marine Science and Engineering Guangdong Laboratory (Zhuhai), Zhuhai, Guangdong 519080, China, Guangdong research center for underground space exploitation technology, Guangzhou, Guangdong 510275, China, Southern Institute of Infrastructure Testing and Rehabilitation Technology, Huizhou, Guangdong 516000, China

Excavation response analysis of prefabricated recyclable support structure for water-rich silt foundation pit

WANG Rui-song[1, 2, 3], GUO Cheng-chao[1, 2, 3, 4], LIN Pei-yuan[1, 2, 3], WANG Fu-ming[1, 2, 3, 4]

1. School of Civil Engineering, Sun Yat-Sen University, Guangzhou, Guangdong 510275, China
2. Southern Marine Science and Engineering Guangdong Laboratory (Zhuhai), Zhuhai, Guangdong 519080, China
3. Guangdong research center for underground space exploitation technology, Guangzhou, Guangdong 510275, China
4. Southern Institute of Infrastructure Testing and Rehabilitation Technology, Huizhou, Guangdong 516000, China

Abstract: The prefabricated recyclable support structure provides a new green support system with economic security, functional coordination and sustainable development for the development of underground space. The physical model test of the foundation pit of a pipe-jacking working well in Zhengzhou city is carried out based on the similarity theory. A three-dimensional fluid-solid coupling model that can differentiate the deformation difference between rigid and flexible components in the support system is established by using the ABAQUS software. The stress and deformation characteristics of support structure in the process of dewatering and excavation are analyzed. The influences of dewatering and excavation on the deformation characteristics of foundation pit are also studied. Results show that in the processes of dewatering and excavation, both the stress and deformation of the primary support structures are all less than those of the design values, while the steel panels are prone to local yield at the position connected with the waist beams. The increment mode of horizontal displacement of retaining pile varies greatly with the processes of dewatering and excavation. With the progress of the dewatering and excavation of the foundation pit, the deformation of the support structure is less affected by dewatering, and the main factor affecting the deformation of the support structure is gradually changing from foundation pit dewatering to foundation pit excavation. The influence of foundation pit dewatering on the surface settlement is greater than that of foundation pit excavation. The surface settlement increases rapidly during the first level of dewatering, with the maximum settlement increment accounting for 44.6%.

Keywords: prefabricated recyclable support structure; foundation pit excavation; foundation pit dewatering; physical model test; finite element analysis

1 Introduction

In foundation pit engineering, the support structure needs to not only ensure the stability and safety of the foundation pit, but also meet the requirements of less space demand, short construction period, less environmental pollution and high recovery rate in urban and rural areas. Therefore, eco-friendly and energy-saving design and construction technology has become an important direction for the future development of foundation pit engineering and underground engineering[1]. Based on the comprehensive consideration of construction cost and safety, functional coordination and sustainable development, Wang et al.[2] developed a composite rigid and flexible impermeable prefabricated recyclable support system. The proposed support system effectively solves the problems existing in the conventional support structure system, such as high cost, low recovery rate, low repeating utilization rate, weak waterproof performance, and high construction control requirement, and it provides a new eco-friendly support structure for the development of underground space. The main structure composition and the corresponding function of this support system are as follows:

(1) Steel frame, which is the primary load-bearing component, with excellent processing performance and stable mechanical properties;

(2) Flexible panel, which is used to disperse water and soil pressures and coordinate the overall forces on the steel frame;

(3) High polymer grouting layer, which is adopted to quickly form a flexible sealed impervious body and block leakage point.

Currently, the support system proposed by Wang et al.[2] has been successfully applied to a number of case projects in North China[3–6], and its excellent support performance has been proven. However, in those case projects, the effect of groundwater was not considered in the process of foundation pit excavation. According to statistical data, the water table in most areas of North China is located at the depths of 1−5 m. Therefore, the groundwater must be drained out during the excavation of prefabricated recyclable foundation pits in North China. Engineering practice has shown that improper treatment of groundwater in the process of foundation pit excavation not only causes engineering accidents, prolonged construction period, and increased construction costs, but also brings about

huge economic losses and adverse impacts on the society[7]. Therefore, it is of great significance to carry out excavation response analysis of prefabricated recyclable support structure for water-rich silt foundation pit. Figure 1 shows the construction processes of the prefabricated recyclable support structure in water-rich areas.
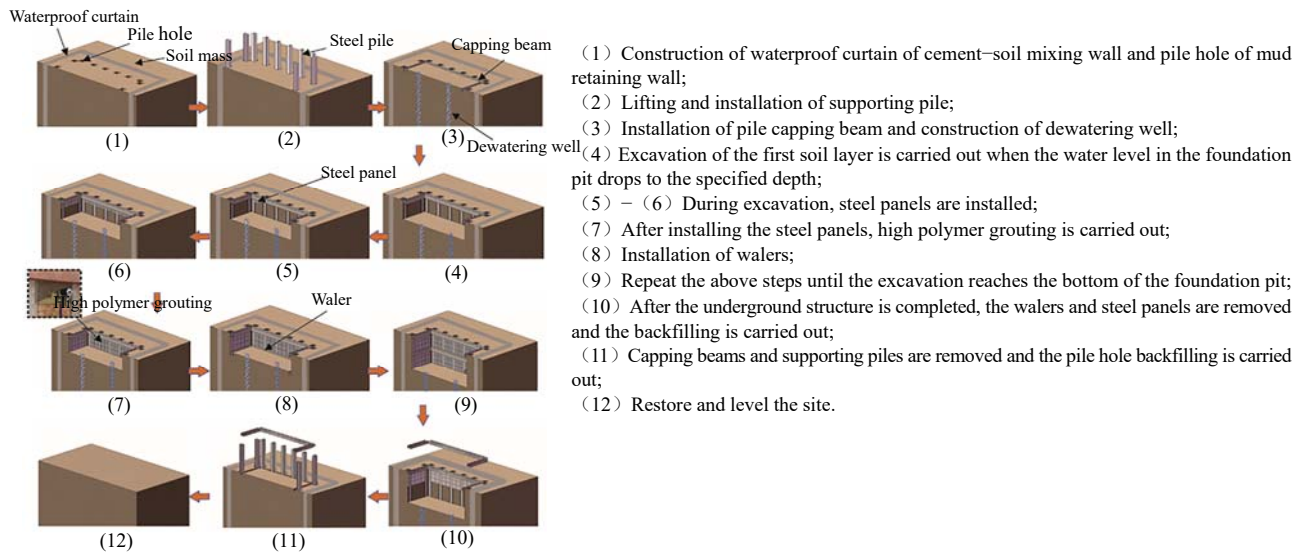

（1）Construction of waterproof curtain of cement−soil mixing wall and pile hole of mud retaining wall;
（2）Lifting and installation of supporting pile;
（3）Installation of pile capping beam and construction of dewatering well;
（4）Excavation of the first soil layer is carried out when the water level in the foundation pit drops to the specified depth;
（5）−（6）During excavation, steel panels are installed;
（7）After installing the steel panels, high polymer grouting is carried out;
（8）Installation of walers;
（9）Repeat the above steps until the excavation reaches the bottom of the foundation pit;
（10）After the underground structure is completed, the walers and steel panels are removed and the backfilling is carried out;
（11）Capping beams and supporting piles are removed and the pile hole backfilling is carried out;
（12）Restore and level the site.

Fig. 1 Construction processes of the prefabricated recyclable support structure

In view of the deformation and failure mechanism of the support structure and surrounding soil in the process of dewatering and excavation of the foundation pit, the failure process of the soil and support structure below the ground surface can be intuitively understood, and the physical and mechanical behaviors and deformation development of the support structure can be revealed by carrying out physical model tests[8−10]. The numerical simulation method[11−14] can be used to analyze the stability, damage, and performance of the support structure and to solve the multi-field coupling problems. For instance, the finite element method (FEM) based on the Biot's theory of consolidation can well simulate the complex boundary conditions and the coupling effect between the stress state of foundation pits and the seepage characteristics of groundwater. In this study, based on the similarity theory, the scaled model test of the dewatering and excavation of the foundation pit of a pipe-jacking working well in Zhengzhou, China was carried out, and a three-dimensional (3D) fluid-solid coupling model considering the entire process of the dewatering and excavation of foundation pit was established using the finite element software ABAQUS. In the established model, the prefabricated construction characteristics of the prefabricated recyclable support structure are considered[2], and the waterproof curtain is designed for water barrier in the process of foundation pit dewatering. In addition, this 3D simulation model can accurately represent the deformation difference between rigid and flexible components in the support structure. In this study, the influence and adverse factors of the dewatering and excavation on the deformation development of the foundation pit are studied, and the simulation results are compared with the measured data to verify the accuracy of the established 3D simulation

model. Based on the 3D finite element model, the stress and deformation characteristics of the main components of support structure, as well as the settlement and deformation mechanism of the soil, are further analyzed at different stages of excavation and dewatering. The research results of this study provide a reference for the application, design optimization and maintenance of this type of prefabricated recyclable support structure in water-rich areas.

2 Physical model test

The physical model test was carried out on a working well of the Yellow River Diversion Trunk Line Project in Zhengzhou[4−6]. The working well was rectangular in shape, with a length of 8.0 m, a width of 5.0 m, and an excavation depth of 11.5 m. According to the regional geological data and site survey results, the exposed thickness of the soil layer within the survey depth of the site is 15.5 m. The soil 0−2.5 m below the ground surface is miscellaneous fill, the soils 2.5−3.6 m and 4.5−14.3 m below the ground surface are loess-like light silty loam, and the soils 3.6−4.5 m and 14.3−15.5 m below the ground surface are loess-like medium silty loam. No groundwater was found during the survey. The prefabricated recyclable support structure was adopted. The pile spacings on the long and short sides of the foundation pit were 1.50 m and 2.25 m, respectively. The diameter of the pile hole was 600 mm, with built-in structural steel HW350. After inserting structural steel into the pile hole, the dry-mixed graded cement gravel equivalent to C20 was used for backfilling. The length of the pile was 15.0 m. Both the capping and waler beams were made of structural steel HW350, and they are connected with structural steel

supporting piles by bolts. The flexible steel panel had a thickness of 5 mm and a strength grade of Q235, which was connected to the supporting piles by welding.

In order to explore the applicability of the prefabricated recyclable support structure in water-rich areas, a suspended waterproof curtain was applied to the outside of the support structure during the model test, and the layout of the foundation pit is shown in Fig. 2.
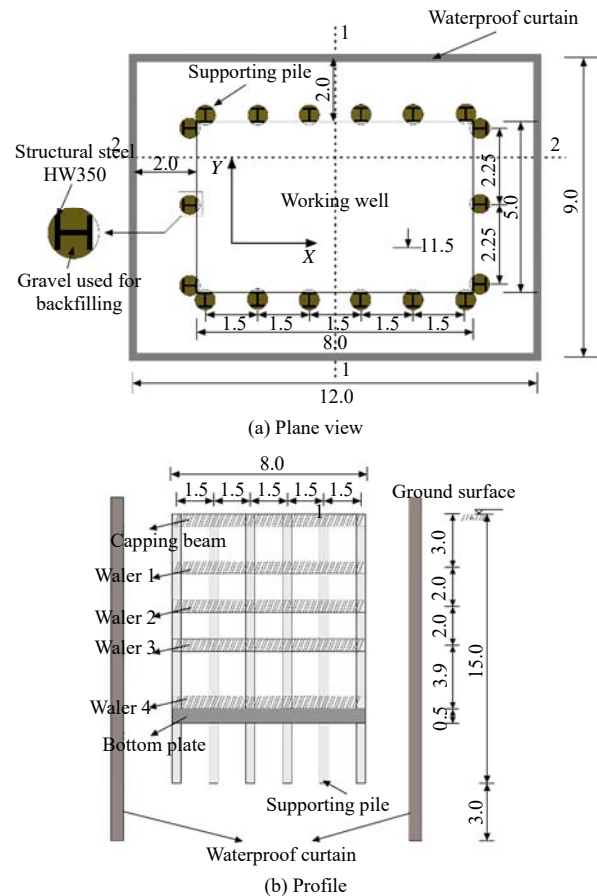
2.1 Similarity ratio of model test

The geometric similarity ratio 1 : 20 was selected for the model test. The similarity criterion equation was obtained according to the dimensional analysis method, and the similarity ratio for each physical parameter was calculated, as listed in Table 1.

2.2 Model box and backfill

A steel frame model box with size of 2.50 m×2.50 m× 1.66 m (length × width × height) was adopted in the model test, and the profile of the model box is shown in Fig. 3(a). To eliminate the effect of soil boundary conditions on the test data, the box wall was treated with a double layer of polytetrafluoroethylene (PTFE) film, and silicone grease lubricant was evenly applied between the two film layers, with a protective layer of 2 mm thick arranged at the outermost layer. During the test, the ratio of the opening area to the total area of the porous partition board was equal to the porosity of the soil by adjusting the number of holes on the porous partition board, which was used to simulate the stable infiltration recharge boundary. The soil used in the test was homogeneous silt, and the parameters of the soil layer were obtained by triaxial consolidation test and shear test in the laboratory, as listed in Table 2. When backfilling was performed, the

backfilling and compaction were carried out layer by layer strictly according to the optimum density of the soil. The total backfilling height was 1.25 m. After the completion of backfilling and compaction, the soil was consolidated under its own weight for 5 months.

(a) Plane view

(b) Profile

Fig. 2　Layout of the foundation pit (unit: m)

Table 1　Similarity ratios for physical model test

Parameters	Geometric parameters			Physico-mechanical parameters							
	Length L	Depth H	Width W	Poisson's ratio v	Unit weight γ	Strain ε	Bending stiffness EI	Horizontal displacement δ	Stress σ	Earth pressure p	Elastic modulus E
Similarity ratio	20	20	20	1	1	1	20^5	20	20	20	20

Note: The similarity of the material's density for the support structure is not strictly considered in this study.

Table 2　Mechanical parameters of soil layer in physical model test

Soil parameters	Depth /m	Unit weight γ/(kN · m^{-3})	Elastic modulus E /MPa	Effective cohesion c' /kPa	Effective internal friction angle ϕ' /(°)	Initial void ratio e_0	Permeability coefficient K /(m · d^{-1})	Critical porosity e_1	Slope of virgin compression line λ	Slope of swelling curve κ	Effective stress ratio M	Poisson's ratio v
Backfill in model test	0−1.25	16.3	25 415	14.52	33.65	0.58	0.18	1.53	0.108	0.004 7	1.359	0.3

Note: The mechanical parameters in the table were obtained through laboratory geotechnical tests on the backfill.

2.3 Dewatering system and support structure model

As shown in Fig. 3, the soil was designed to be saturated with water during the test. In order to simulate the actual dewatering process of the foundation pit, a pumping system consisting of automatic pumping pumps, flowmeters, filters, plastic hoses and asbestos mesh was used. The PVC pipe with an outer diameter of 18 mm and an inner diameter of 16 mm was employed in the dewatering and observation wells. The length was set to 725 mm, and

the filter sections were set according to the range of dewatering depth. The design depth of the suspended waterproof curtain was 0.9 m, which met the technical specification for building foundation pit support where the bottom end of the waterproof curtain was located in the silt aquifer[15]. It should be noted that in this model test, the effect of groundwater recharge on the dewatering and excavation of the foundation pit was not studied, and no recharge well was set during the test. The support

structure and dewatering system were both first assembled in the form of prefabrication, and then buried in the soil layer together with the backfill. That is, before the dewatering and excavation of the foundation pit, the construction of the support structure and dewatering wells have been completed.
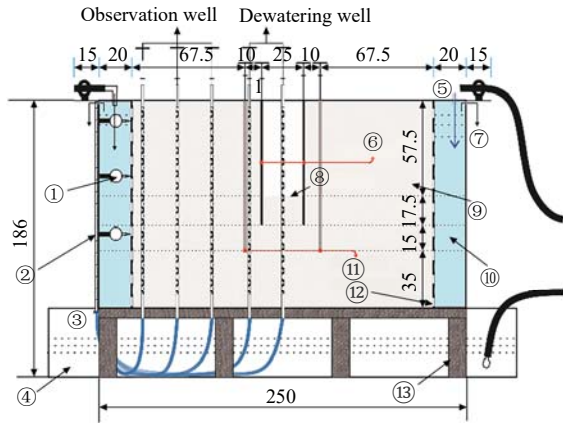
①Dial gage; ②Water level observation meter; ③Bottom plate; ④Water storage tank; ⑤Direction of water intake; ⑥Support structure; ⑦Overflow vent; ⑧Final excavation face; ⑨Backfilling box; ⑩Water recharge tank; ⑪Waterproof curtain; ⑫Perforated steel partition board; ⑬Base bracket

(a) Model box
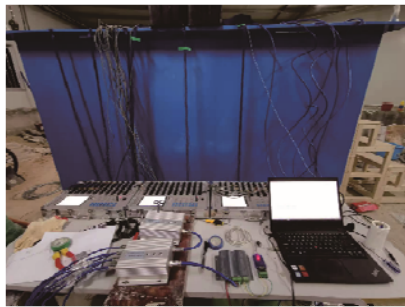
(b) Photo

Fig. 3   Physical model box system (unit: cm)

As shown in Fig. 4(a), the duralumin, rubber plate and hot melt adhesive were adopted to simulate the steel frame, steel panel and high polymer grouting layer in the support structure model, where D_1 and D_2 are the monitoring paths for surface settlement. The components of the support structure were bonded with epoxy resin, and the dimensions of each component are listed in Table 3.

2.4 Monitoring devices

(1) Distributed optical fiber. The horizontal displacement of the supporting pile was measured by OSI distributed fiber optical sensors. The test process is shown in Fig. 4.

(2) Strain gage. The strain changes of the supporting piles and flexible panels were monitored by waterproof strain gages, with electrical resistance of 119.9±0.3 Ω and sensitivity coefficient of 1.96±1%.

(3) Single-point settlement meter. The ground surface settlement around the foundation pit was measured by using a single-point settlement meter and a fixed dial gage, as shown in Fig. 4(b), with a measurement accuracy of 0.01 mm.
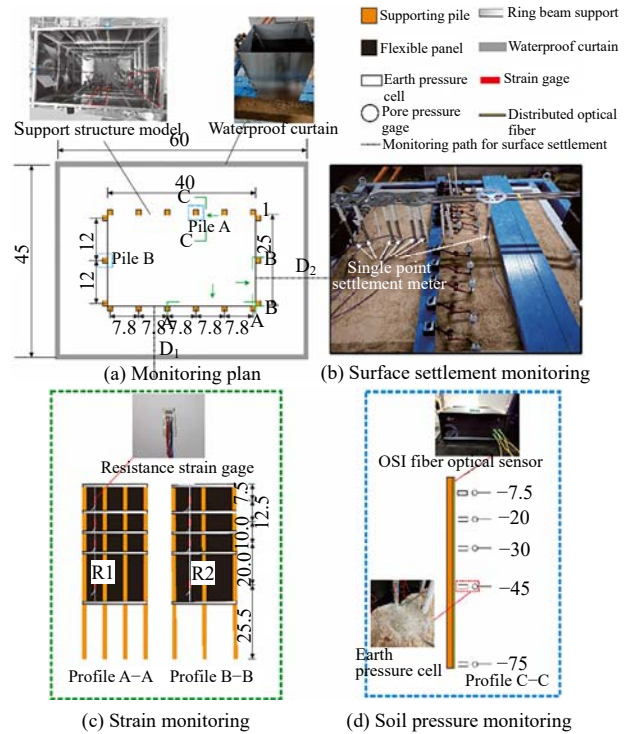

Fig. 4   Layout of monitoring points in model test (unit: cm)

Table 3   Material parameters in physical model test

Support component	Model material	Model size /m	Calculated values of similarity ratio	Error rate /%
Supporting pile	Duralumin	$L0.01 \times W0.01 \times H0.75$	$1/(3.24 \times 10^6)$	1.25
Wale(X direction)	Duralumin	$L0.4 \times W0.008\ 2 \times H0.008\ 2$	$1/(3.19 \times 10^6)$	0.31
Waler(Y direction)	Duralumin	$L0.25 \times W0.008\ 2 \times H0.008\ 2$	$1/(3.19 \times 10^6)$	0.31
Flexible panel	Rubber plate	$T0.003 \times L \times W$	$1/(3.12 \times 10^6)$	0.09
Waterproof curtain	Steel plate	$L0.6 \times W0.45 \times H0.9 \times T0.001\ 5$	$1/(2.91 \times 10^6)$	9.06

Note: T is the thickness, and the length and width of the rubber plate are determined according to the actual situation.

(4) Earth pressure cell. To study the earth pressure acting on the supporting piles, the resistivity-type miniature earth pressure cells were arranged behind some model piles, as shown in Profile C-C in Fig. 4(d). The dimensions of the earth pressure cell were 35 mm in diameter and 7 mm in thickness.

2.5 Test procedures

There are two types of model tests in this study, i.e. ordinary excavation and excavation with dewatering. The variables in these two model tests are the presence or absence of groundwater and waterproof curtain.

In the model, the methods of dewatering by stages and stepwise excavation were adopted. The depth of dewatering at each stage was identified by the water head change of the observation well. The dewatering duration at each stage was about 3.5 h. After the water table dropped to the specified depth, the foundation pit excavation was carried out. The first excavation depth was 15.0 cm, the second and third excavation depths were 10.0 cm, and the last excavation depth was 22.5 cm. After the completion

of each excavation, the next excavation was carried out until the displacement of the pile was stable. The processes of the dewatering and excavation of foundation pit are shown in Fig. 5.
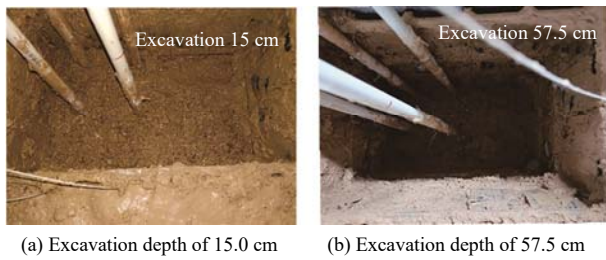

(a) Excavation depth of 15.0 cm   (b) Excavation depth of 57.5 cm

Fig. 5 Dewatering and excavation of the foundation pit with prefabricated recyclable support structure

3 Numerical simulation

In this study, the finite element software ABAQUS was used to establish a 3D fluid-solid coupling model. In order to reduce the influence of boundary conditions on the calculation area, the distance from the edge of the foundation pit to the model boundary was set to be greater than $4.3H_{em}$ (H_{em} is the maximum excavation depth of the foundation pit), which exceeded the influence radius of the dewatering well calculated by the Sichardt formula[16]. As shown in Fig. 6, the size of the model is 120 m×120 m×40 m (length × width ×height), and dense mesh and sparse mesh are generated inside and outside the model. This soil model contains a total of 34 188 elements.

(a) Finite element meshing

(b) Support structure and waterproof curtain

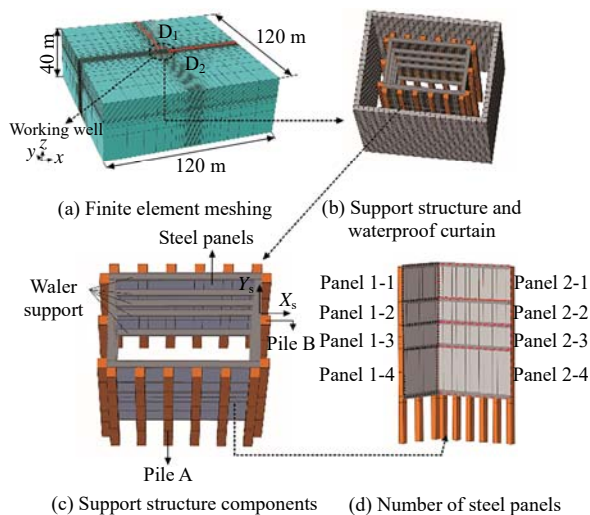(c) Support structure components

(d) Number of steel panels

Fig. 6 Finite element model

3.1 Soil constitutive model and model parameters

In this study, the elasto-plastic deformation behaviour of the soil was simulated by the modified Cambridge model, which can well reproduce the soil deformation characteristics under repeated loading and unloading in the process of dewatering and excavation. The parameters used in the soil model are listed in Table 2. The main load-bearing component of the prefabricated support structure is the structural steel HW350. On the premise

that the similarity ratio of the material in the model was satisfied, the supporting pile around the working well was simplified into a rectangular steel pile by adopting the principle of equal bending stiffness[17]. The calculation process can be found in Guo et al.[5]. Detailed parameters of each supporting component are listed in Table 4.

Table 4 Parameters of support structure in finite element model

Supporting component	Model size /m	Unit weight $\gamma/(\mathrm{kN \cdot m^{-3}})$	Elastic modulus E /MPa	Poisson's ratio v
Supporting pile	$L0.5×W0.5×H15$	32.5	$36.2×10^3$	0.25
Waler	Structural steel HW350	78	$210×10^3$	0.3
Steel panel 1-1	$T0.005×L5.0×W3.0$	78	$210×10^3$	0.3
Steel panel 2-1	$T0.005×L8.0×W3.0$	78	$210×10^3$	0.3
Steel panel 1-2/1-3	$T0.005×L5.0×W2.0$	78	$210×10^3$	0.3
Steel panel 2-2/2-3	$T0.005×L8.0×W2.0$	78	$210×10^3$	0.3
Steel panel 1-4	$T0.005×L5.0×W4.0$	78	$210×10^3$	0.3
Steel panel 2-4	$T0.005×L8.0×W4.0$	78	$210×10^3$	0.3
Waterproof curtain	$T0.5×L8.0×W4.0× H12.0$	25	$15.6×10^3$	0.2

3.2 Contact model and boundary conditions

The friction model was adopted for the contact surface between the support structure and the soil. The normal extrusion behaviour is controlled by the "Hard" contact model, i.e. it is assumed that the contact surface can transfer infinite pressure but not tension. The tangential friction behaviour is controlled by the "Penalty" friction contact model, which follows Coulomb's elasto-plastic friction law. Both the friction coefficient μ and the ultimate shear slip parameter γ_{crit} follow the ideal elasto-plastic Coulomb friction model. In the model, for the interface between the support structure and the soil, $\mu = 0.35$ and $\gamma_{crit} = 5$ mm; for each supporting component, $\mu = 0.12$ and $\gamma_{crit} = 5$ mm. The surface contact was established between the passive side of the support structure and the excavated soil of each layer. The "Tie" contact model was adopted for the contact between the bottom of the supporting pile and the soil, between the supporting pile and the waler, and between the supporting pile and the steel plate, i.e. it is assumed that no relative sliding and deformation occur in the binding area.

In the case of ordinary excavation, the horizontal displacement was restricted by the outer boundary of the model, the displacement in three directions was restricted by the bottom of the model, and the free boundary condition was applied to the upper surface of the model. In the case of excavation with dewatering, the dewatering of the foundation pit was simulated by setting the boundary of drainage-only flow (DOF) at the cross-section of the water flow. The outer boundary of the model constrained the horizontal displacement, and the constant head recharge was set. The bottom surface of the model was set as the

impermeable surface constrained in the horizontal and vertical directions, and the DOF boundary was set on the upper surface of the model.

3.3 Simulation of dewatering processes

In the inp file of ABAQUS software, the ground surface and dewatering well wall are defined as the seepage boundaries of DOF, which can simulate the effect of seepage on the foundation pit in the process of dewatering by stages. Assuming that the pore pressure on the DOF boundary is positive, we have

$$v_n = \begin{cases} k_s \ p_w, \ p_w > 0 ; \\ 0, \quad p_w \leqslant 0 \end{cases} \quad (1)$$

where v_n is the velocity of water flow; k_s is the coefficient of permeability; and p_w represents the pore pressure. v_n is proportional to p_w and k_s. When the pore pressure is negative, the fluid does not enter the interior of the region.

This means that groundwater can only flow from the soil into the dewatering well, rather than from the dewatering well into the soil, which is consistent with the actual dewatering process. k_s, as a key control parameter of the DOF boundary, can be derived from the following equation, and the derivation process can be found in the literature[12−13]:

$$k_s = \frac{A \sum_{i=1}^{n} u h_i}{\pi D L_p N t p_w} \quad (2)$$

where A is the area of foundation pit; u is the specific water yield of soil layer ($u = 0.15$ in this study); D is the radius of dewatering well; h_i is the aquifer thickness within the filter tube range; N is the number of dewatering wells; t is the dewatering time; and L_p is the length and width of the filter tube layout (m).

3.4 Numerical simulation method

When assigning the type of support structure element, C3D8 solid linear elements were used for the supporting pile, waterproof curtain, and bottom plate. According to the working conditions, the soil adopted the C3D8 element for ordinary excavation and the C3D8P pore pressure element for excavation with dewatering. The S4 shell element was used for the steel panel, and the B31 beam element was used for ring beam support. The foundation pit was divided into four stages of excavation. Prior to the excavation of each stage, the dewatering was carried out in the foundation pit in advance, and then the soil element required to be excavated in the next layer was "killed" and the corresponding supporting component elements were "activated". Table 5 shows the simulated working conditions of the whole process of the dewatering and excavation of the foundation pit.

4 Validation of 3D finite element model

Since the support was installed before excavation in the model test, the numerical simulation here also followed the procedure of installing the support first and then carrying out the excavation. The subsequent excavation response

analysis of the foundation pit during dewatering was numerically analyzed according to the actual working conditions in Table 5.

Table 5   Steps of numerical simulation

Step	Stage	Simulated construction content
1	Initial	Equilibrium of initial in situ stress (remove all the elements and contacts outside the original soil)
2		Completion of the construction of the waterproof curtain, steel pile and dewatering well (remove the soil elements at the waterproof curtain and steel pile, and activate the elements of waterproof curtain and steel pile and their corresponding contacts)
3	1	Initiation of first dewatering stage. The dewatering lasted for 1.5 d and the water level dropped to about 4.5 m
4		Completion of capping beam construction. The first excavation step was carried out to −3 m. The construction of the first waler beam and the first steel panel was completed
5	2	Initiation of second dewatering stage. The dewatering lasted for 0.5 d and the water level dropped to about 2.0 m
6		The second excavation step was carried out to −5 m. The construction of the second waler and the second steel panel was completed
7	3	Initiation of third dewatering stage. The dewatering lasted for 0.5 d and the water level dropped to about 1.5 m
8		The third excavation step was carried out to −7 m. The construction of the third waler and the third steel panel was completed
9	4	Initiation of fourth dewatering stage. The dewatering lasted for 1.5 d and the water level dropped to about 5.0 m
10		The fourth excavation step was carried out to −11.5 m. The construction of the fourth waler and the fourth steel panel was completed

Figure 7 shows the comparisons between the measured values of the model test and the simulated values of the finite element model for pile A at different stages of dewatering and excavation. It can be seen that the simulated values from the finite element model are relatively close to the measured values, and the overall deformation trend of the pile obtained by the two methods is also basically consistent. At the early stage of dewatering and excavation, pile A showed cantilever-type deformation. When the first excavation stage was completed, the maximum displacement at the top of pile A was 5.2 mm. When the second excavation stage was completed, the deformation mode of pile A began to shift to "convex" form as the support gradually took effect. It showed that with the increase of the excavation depth during dewatering, the increasing trend of pile top deformation slowed down, the maximum horizontal displacement of pile body rapidly increased, and the maximum lateral displacement position of pile body deepened continuously. When the excavation of the foundation pit was completed, the maximum horizontal displacement of pile A, located at the position of $0.7H_{em}$, reached 11.3 mm.

Figure 8 shows the comparisons of the surface settlement at the end of excavation obtained by various methods (without considering the influence of groundwater), where d is the distance from the wall of the foundation pit, H_e is the excavation depth of the foundation pit, δ_v is the surface settlement, and δ_m is the maximum surface

(a) Dewatering of foundation pit
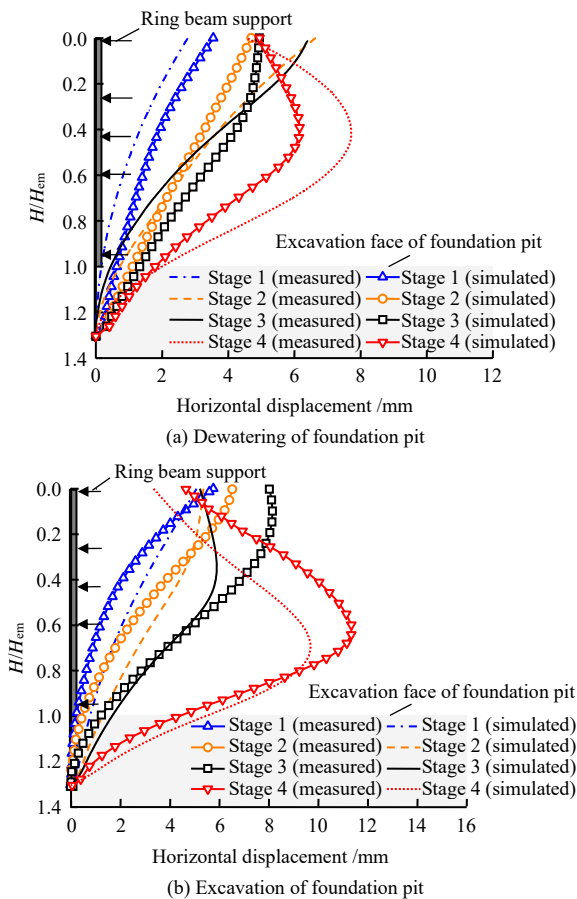

(b) Excavation of foundation pit

Fig. 7 Comparisons between simulated and measured data of horizontal displacement for pile A during dewatering and excavation

settlement. It can be seen that the simulated results of surface settlement were in good agreement with the measured values, and the simulated values were slightly less than the measured values. It is also found that the simulated and measured values of the surface settlement in D_1 and D_2 directions are in good agreement with the trend of the predicted curve of Guo et al.[5] but are greatly different from the trend of the empirical predicted curve of Hsieh et al.[18] and Li et al.[19]. This is because the deformation difference between rigid and flexible components in the structure system leads to a sharp increase in soil settlement behind the steel plate and the appearance of the settlement in a vortex form (see Fig. 8(b)). The positions of the maximum surface settlement are all located at the positions less than $0.1H_e$.

Figure 9 shows the comparisons between the measured and simulated values of the strain of the flexible panel after the completion of foundation pit excavation. It can be seen that the variation trend of the measured and simulated values is basically consistent, both showing that the strain of the flexible panel increases gradually with the increase of depth. On the monitoring path R1, the maximum strain obtained from the model test is $524×10^{-6}$, and the maximum strain by numerical simulation is $478×10^{-6}$, all located at the positions of $0.9H_{em}$. On the monitoring path R2, the maximum strain obtained from the model

test is $518×10^{-6}$, which is basically consistent with the maximum simulated value at the same location ($585×10^{-6}$).
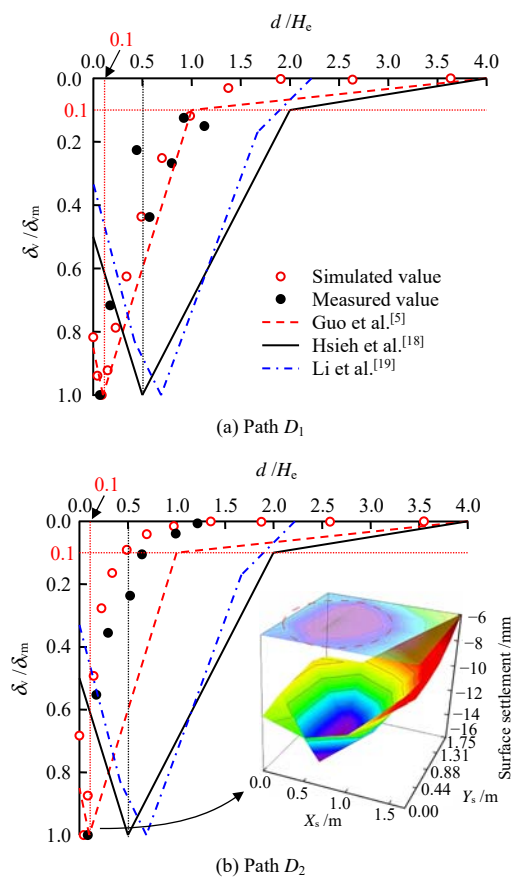

(a) Path D_1

(b) Path D_2

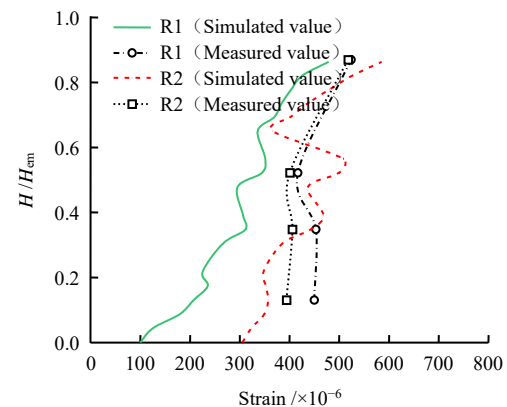**Fig. 8 Comparisons of surface settlement data**

Fig.9 Comparisons of steel panel strain based on monitoring data

# 5 Excavation response of foundation pit under dewatering

Through the comparisons between the measured data with the numerical results mentioned above, the 3D simulation model established in this study can well reproduce the deformation behaviour of structure components and surrounding soil. On the basis of this 3D model, the excavation response analysis of the foundation pit with prefabricated recyclable support structure during dewatering was carried out.

5.1 Stress analysis of supporting pile during dewatering and excavation

Figure 10 shows the variation trends of the maximum von Mises stress of the supporting pile and the pile bending moment at each stage of the dewatering and excavation of the foundation pit. According to the von Mises yield criterion[20], the most dangerous area of the support structure in the model can be quickly identified.
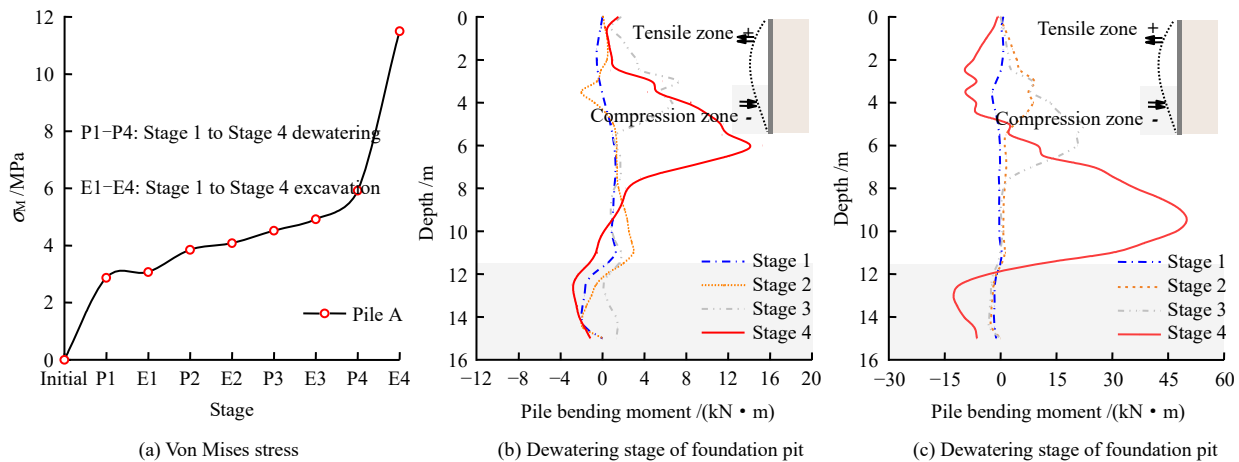
Fig. 10 **The maximum von Mises stresses (σ_{max}) and bending moments of pile A at different dewatering and excavation stages**

As shown in Fig. 10, when the excavation of the foundation pit was completed, the σ_M of the supporting pile was 11.5 MPa, which was much smaller than its design strength (305 MPa). During the dewatering and excavation stages, the positive and negative bending moments of the pile body indicated that the passive side of the supporting pile was in a tension and compression state. At the end of the first dewatering and excavation stage, the pile body generated a small positive bending moment. As the dewatering and excavation proceeded, the absolute value of the pile bending moment increased continuously. A reverse bending point appeared near the supporting position, and the position of the reverse bending point moved downward continuously. At the early stage of dewatering and excavation, the pile bending moment was less affected. At the end of the third excavation stage, the maximum bending moment of the pile body was only 20.6 kN·m. The fourth dewatering and excavation stage has the most prominent influence on the pile body. When the excavation of the foundation pit was completed, the maximum bending moment of pile A was 49.8 kN·m, far smaller than the maximum allowable design bending moment (724.5 kN·m). The analysis results indicate that the supporting piles in this support structure system have strong stability, effectively ensuring the recycling rate of the pile.

5.2 Stress and deformation analysis of steel panel

As the flexible components in the support system, steel panels often generate large deformation and stress. As shown in Fig. 11, this section selects the position where the steel panel has the largest deformation subjected to stress (the depth range from 9 m to 11 m) to analyze the variations of the horizontal displacement and von Mises stress of the steel panel during the dewatering and excavation of the foundation pit.

Figure 12 shows the variation curves of the von Mises stress and horizontal displacement of the steel panel at the end of the excavation of the foundation pit, where *R*
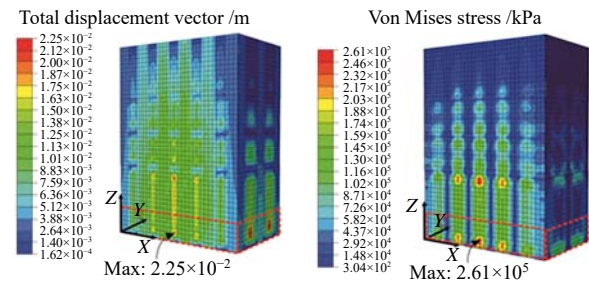
Fig. 11 **Contours of deformation and stress of steel panels**

is the length along the circumference of the working well. As shown in Fig. 12, in the *X* direction of foundation pit, the maximum horizontal displacement of the steel panel is 22.5 mm, larger than that in the *Y* direction (20.4 mm), but both are smaller than the early-warning value. It is worth noting that in the *X* direction of the foundation pit, the maximum von Mises stress in the local area of the steel panel reaches 261 MPa, exceeding the yield strength of Q235 steel (215 MPa), while in the *Y* direction, the maximum von Mises stress is only 120 MPa. This could be attributed to the fact that the deformation difference among the supporting pile, steel support and steel panel results in the local stress concentration of the steel panel at the connection position. Therefore, in the process of dewatering and excavation, the connection between the steel panel and the supporting component should avoid the factors that might cause the stress concentration of the steel panel, such as sharp corners and welding defects, or the Q345 steel plate should be used for construction.

5.3 Influence of dewatering and excavation on the deformation of supporting piles

In practical engineering, the dewatering and excavation of the foundation pit is a continuous process, and the induced deformation of support structure and ground has a hysteretic phenomenon, thus it is difficult to obtain accurate values during measurement. However, with the
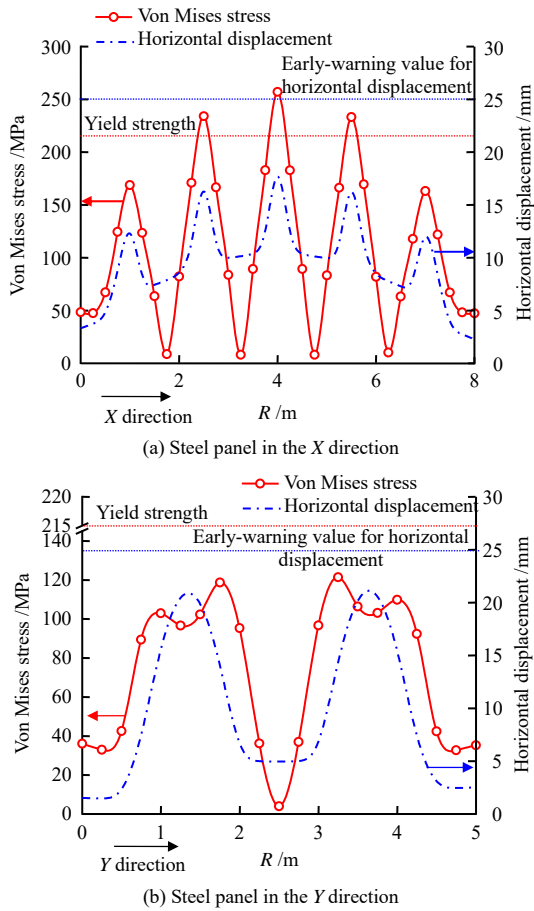
(a) Steel panel in the X direction

(b) Steel panel in the Y direction

Fig. 12 Von Mises stresses and horizontal displacements of steel panels

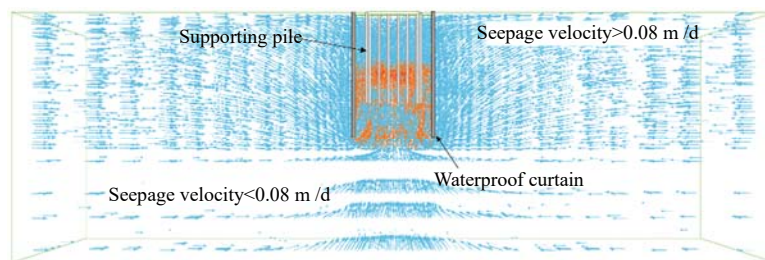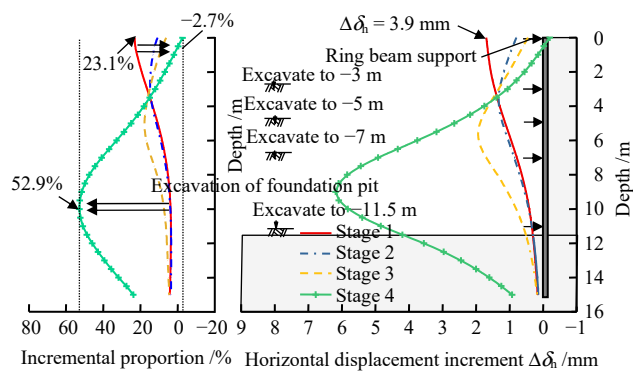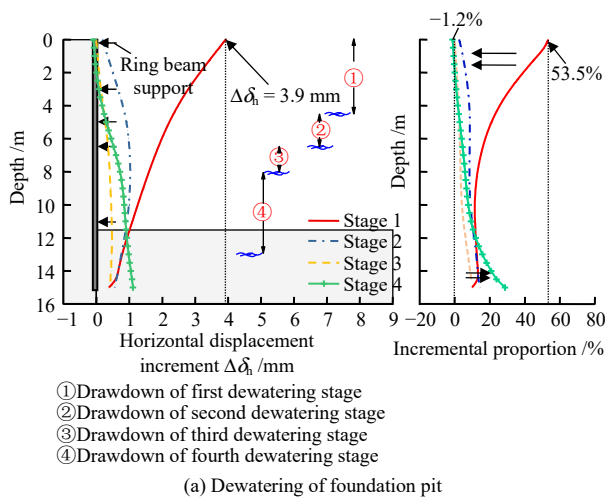use of the numerical model for the water−soil coupling simulation, the deformation caused by excavation and dewatering can be easily distinguished. Therefore, the influences of dewatering and excavation on the deformation of supporting pile A are explored by establishing a 3D fluid-solid coupling model to analyze the change of horizontal displacement increment $\Delta\delta_h$ of supporting pile A at different stages.

Figure 13 shows the variations of the horizontal displacement increment and the corresponding increment proportion of pile A at each stage of dewatering and excavation, where the positive value represents the increase of horizontal displacement and the negative value represents the decrease of horizontal displacement.

As shown in Fig. 13(a), when the first dewatering stage was completed, the overall change of $\Delta\delta_h$ was in the form of cantilever, and $\Delta\delta_h$ of the pile top was 3.9 mm, accounting for about 53.5%. As the pore water pressure of the soil in the foundation pit dissipated further, the lateral pressure on the pile became smaller and smaller, and the installation of the support structure effectively improved the ability of the pile to resist deformation. Therefore, during the second and third dewatering stages, $\Delta\delta_h$ of the upper part of the pile body showed a gradually decreasing trend. On the contrary, with the progress of dewatering, under the action of horizontal seepage force, the lateral pressure in the active zone of the pile gradually increased, exacerbating the deformation of the pile towards the passive zone (in the pit). This process finally resulted in a gradually increasing trend of horizontal displacement increment near the pile bottom. When the fourth dewatering stage was completed, $\Delta\delta_h$ of the upper part of the pile body was −0.1 mm, and $\Delta\delta_h$ of the pile bottom was 1.1 mm. The variation trend of $\Delta\delta_h$ changed from the cantilever

①Drawdown of first dewatering stage
②Drawdown of second dewatering stage
③Drawdown of third dewatering stage
④Drawdown of fourth dewatering stage

(a) Dewatering of foundation pit

(b) Excavation of foundation pit

(c) Seepage field around foundation pit

Fig. 13 Variations of horizontal displacement increment of pile A and velocity vectors of seepage field around foundation pit

form to the kicking form.

As shown in Fig. 13(b), during the first excavation stage, the variation trend of $\Delta\delta_h$ of the pile remained in a cantilever form, and $\Delta\delta_h$ of the pile top was 1.7 mm, accounting for about 23.1%. As the excavation of the foundation pit proceeded, $\Delta\delta_h$ of the upper part of the pile ($H<3$ m) gradually decreased, while $\Delta\delta_h$ of the lower part of the pile ($H>3$ m) gradually increased. The variation trend of $\Delta\delta_h$ of the pile changed from the original cantilever form to the convex form. When the excavation of the foundation pit was completed, $\Delta\delta_h$ of the pile top decreased to a negative value, accounting for about -2.7%. During the fourth excavation stage, the maximum cumulative horizontal displacement increment of the lower part of the pile was 6.2 mm, accounting for about 52.9%.

The analysis results indicated that at the initial stage of dewatering and excavation, dewatering had the greatest influence on the horizontal displacement of the pile top. At Stages 2 and 3, the influence of foundation pit dewatering on pile deformation was similar to that of foundation pit excavation. As the support structure gradually took effect, the influence of dewatering on the structure deformation became weaker and weaker, and the excavation of the foundation pit gradually became the main factor affecting the horizontal displacement of supporting piles.

5.4 Influences of dewatering and excavation of foundation pit on surface settlement

As shown in Fig. 14, the construction of the waterproof curtain divided the soil surrounding the prefabricated support structure into two areas, i.e. the transition zone between the prefabricated support system and the waterproof curtain wall, and the outer area of the foundation pit outside the waterproof curtain wall. In this section, the influences of the dewatering and excavation of the foundation pit on surface settlement are analyzed by studying the soil settlement and its increment along the D1 path at each stage of dewatering and excavation.

As can be seen from Fig. 14, the soil settlement in the transition zone is in a "concave" shape, characterized by a smaller settlement in the immediate vicinity of the wall and a larger settlement in the middle. This is due to the frictional restriction between the soil and the retaining wall[13]. The maximum settlement was 39.2 mm. For the outer area of the foundation pit, due to the lack of any support during the construction process of the waterproof curtain wall, as the main retaining component, the prefabricated support structure, together with the soil in the transition zone, played a certain supporting role in the waterproof curtain wall. Therefore, the deformation of the waterproof curtain wall presented a transition state from cantilever form to convex form. Combined with the prediction of Ou et al.[21] and Clough et al.[22] on the deformation of the wall with/without support structure and the surface settlement curve, the surface settlement behind the waterproof curtain wall tended to be in a state of transition from triangular settlement to concave settlement. When the excavation of the foundation pit was completed, the maximum settlement of the soil outside the foundation pit was 16.4 mm.
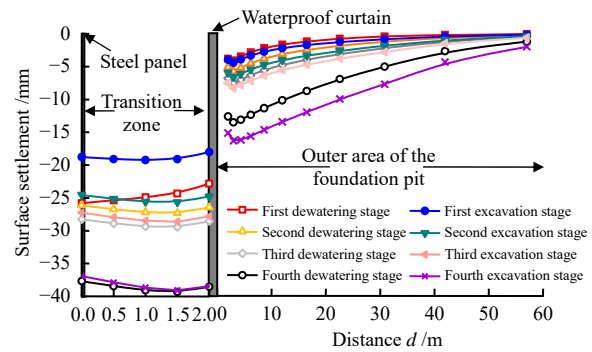

Fig. 14 Surface settlements along the D₁ monitoring path

Figure 15 shows the variation trends of surface settlement increment $\Delta\delta_v$ at each stage of dewatering and excavation, where the positive value represents settlement, the negative value represents rebound, ΔH_e is the excavation depth of each stage, and ΔH_w is the dewatering drawdown. As can be seen from Fig. 15, as the foundation pit dewatering progressed in the transition zone, the soil settlement further intensified along with the continuous dissipation of pore water pressure in the soil. The excavation of the foundation pit caused a certain rebound of the soil. Correspondingly, the soil outside the foundation pit exhibited intensified settlement during both dewatering and excavation, and the dewatering of the foundation pit was the main factor causing soil settlement. It is believed that the dewatering of the foundation pit has a great influence on soil consolidation, seepage field changes and the deformation of the retaining structure, while the excavation of the foundation pit only has a significant influence on the deformation of the retaining structure. Since the surface settlement in the process of foundation pit dewatering is jointly affected by soil consolidation, seepage and deformation of the retaining structure, the foundation pit dewatering has a greater influence on the settlement of the soil outside the wall.
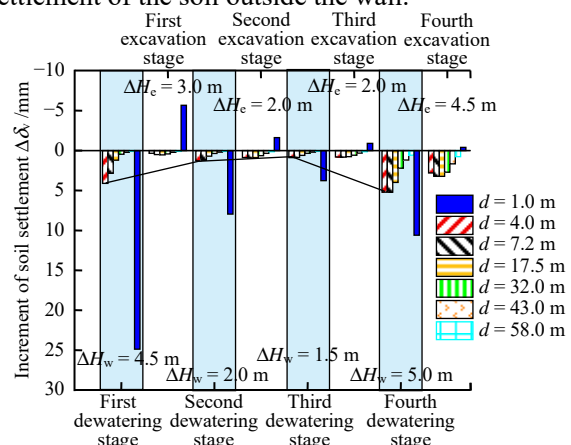

Fig. 15 Variations of surface settlement increment along the D₁ monitoring path at each stage of dewatering and excavation

6 Conclusions

In order to explore the applicability of the prefabricated recyclable support structure in the water-rich silty soil layer, this study conducted the model test and numerical simulation on a working well of the Yellow River Diversion

Trunk Line Project in Zhengzhou. The stress and deformation characteristics of the prefabricated recyclable support structure and the surrounding soil in the processes of the excavation and dewatering of foundation pit were analyzed. The main conclusions are drawn as follows:

(1) During the excavation and dewatering of the foundation pit, the maximum von Mises stress and horizontal displacement of the steel panel are greater than those of the support pile, but both of them are smaller than the design allowable values. It should be noted that the steel panel is prone to local yielding at the position where it is connected to the support. Therefore, it is suggested that the factors that might cause the stress concentration of the steel panel, such as sharp corners and welding defects, should be avoided in the actual construction process, or the Q345 steel plate should be used for construction.

(2) During the first dewatering and excavation stage, the cantilever-form lateral displacement of the supporting pile develops rapidly, and the cumulative horizontal displacement increment of the pile top accounts for up to 76.6%. The dewatering at the later stage results in the kicking-form lateral displacement of the supporting pile, and the excavation at the later stage causes the internal convex-form lateral displacement of the supporting pile. As the support structure gradually takes effect, the influence of dewatering on the structure deformation becomes weaker and weaker, and the excavation of the foundation pit gradually becomes the main factor affecting the horizontal displacement and deformation of supporting piles. During the fourth excavation stage, the cumulative horizontal displacement increment of the lower part of the pile accounts for up to 52.9%.

(3) For the foundation pit with prefabricated recyclable support structure, the installation of waterproof curtain changes the size and range of the soil settlement inside and outside the wall, which is manifested as a "concave" settlement of the soil in the transition zone, and a transition from triangular to "concave" settlement of the soil in the outer zone of the foundation pit. The dewatering of the foundation pit causes the settlement and deformation of the soil in both the transition zone and the outer area of the foundation pit, while the excavation of the foundation pit causes the rebound of the soil in the transition zone and the settlement and deformation of the soil outside the pit.

(4) During the excavation and dewatering of the foundation pit, the surface settlement is jointly affected by soil consolidation, seepage and deformation of the retaining structure. Compared to the excavation of the foundation pit, the cumulative surface settlement caused by foundation pit dewatering is greater than that induced by excavation. During the first dewatering stage, the surface settlement increases rapidly with the increase of dewatering depth, with the maximum increment of surface settlement accounting for up to 44.6%. Therefore, it is recommended to avoid excessive dewatering at one time before the excavation of the foundation pit.

References

[1]   ZHENG Gang, ZHU He-hua, LIU Xin-rong, et al. Control of safety of deep excavations and underground engineering and its impact on surrounding environment[J]. China Civil Engineering Journal, 2016, 49(6): 1−24.

[2]   WANG Fu-ming, FANG Hong-yuan, PAN Yan-hui, et al. Design and construction method of a flexible prefabricated recyclable rectangular working shaft support structure, China: CN 201811095566.1[P]. [2018-12-21].

[3]   PAN Y, FANG H, LI B, et al. Stability analysis and full-scale test of a new recyclable supporting structure for underground ecological granaries[J]. Engineering Structures, 2019, 192: 205−219.

[4]   GUO C, YE J, ZHAO C, et al. Mechanical and deformation characteristics of composite assembled supporting structure[J]. Geotechnical Research, 2020, 7(4): 230−243.

[5]   GUO C, WANG R, LIN P, et al. Numerical analyses of a prefabricated retaining system for foundation pits in silt soils[J]. Geotechnical Research, 2020, 7(3): 173−190.

[6]   WANG Rui-song, GUO Cheng-chao, CAO Ding-feng, et al. Deformation characteristics of flexible support structure in silt foundation pit[J]. Science Technology and Engineering, 2021, 21(5): 2011−2018.

[7]   XIANG Xing-hua. Study on influences of foundation pit excavation and precipitation on stresses in support structure and land deformations[D]. Taiyuan: Taiyuan University of Technology, 2013.

[8]   XUE Li-ying, YANG Bin, LIU Feng-min, et al. Model test system for groundwater seepage in foundation pit engineering[J]. Chinese Journal of Geotechnical Engineering, 2017, 39(Suppl.1): 126−130.

[9]   WANG J, DENG Y, MA R, et al. Model test on partial expansion in stratified subsidence during foundation pit dewatering[J]. Journal of Hydrology, 2018, 557: 489−508.

[10]   CENG Chao-feng, XUE Xiu-li, SONG Wei-wei, et al. Mechanism of foundation pit deformation caused by dewatering before soil excavation: an experimental study[J]. Rock and Soil Mechanics, 2020, 41(9): 2963−2972.

[11]   SHEN S, MA L, XU Y. Interpretation of increased deformation rate in aquifer IV due to groundwater pumping in Shanghai[J]. Canadian Geotechnical Journal, 2013(11): 1129−1142.

[12]   ZHENG Gang, ZENG Chao-feng. Lateral displacement of diaphragm wall by dewatering of phreatic water before excavation[J]. Chinese Journal of Geotechnical Engineering, 2013, 35(12): 2154−2163.

[13]   ZHENG G, ZENG C, DIAO Y, et al. Test and numerical research on wall deflections induced by pre-excavation dewatering[J]. Computers and Geotechnics, 2014: 244−256.

[14]   LI Lian-xiang, HU Feng, HU Xue-bo, et al. Development and application of new type of assembly recyclable soil nailing for foundation pit engineering[J]. Rock and Soil Mechanics, 2017, 38(Suppl.1): 113−122.

[15]   Ministry of Housing and Urban-Rural Development of People's Republic of China. JGJ120−2012 Technical specification for building foundation pit support[S]. Beijing: China Architecture & Building Press, 2012.

[16]   CASHMAN P M, PREENE M. Groundwater lowering in construction: a practical guide to dewatering[M]. [S. l.]: Taylor & Francis Group, 2012.

[17]   LIU Jian-hang, HOU Xue-yuan. Excavation engineering handbook[M]. Beijing: China Architecture & Building Press, 1998.

[18]   HSIEH P, OU C. Shape of ground surface settlement profiles caused by excavation[J]. Canadian Geotechnical Journal, 1998, 35(6): 1004−1017.

[19]   LI D, LI Z, TANG D. Three-dimensional effects on deformation of deep excavations[J]. Proceedings of the Institution of Civil Engineers-Geotechnical Engineering, 2015, 168(6): 551−562.

[20]   CHEN Ming-xiang. Mechanics of elasticity and plasticity[M]. Beijing: Science Press, 2007.

[21]   OU C, HSIEH P, CHIOU D. Characteristics of ground surface settlement during excavation[J]. Canadian Geotechnical Journal, 1993, 30(5): 758−767.

[22]   CLOUGH G W, O'ROURKE T D. Construction induced movements of in situ walls[J]. Specialty Conference on Design and Performance of Earth Retaining Structure, 1990, 25: 439−470.